

## Formation of ordered cobalt nanowire arrays in the mesoporous silica channels\*

Marina V. Chernysheva<sup>1</sup>, Nina A. Sapoletova<sup>1</sup>, Andrei A. Eliseev<sup>1,‡</sup>, Alexey V. Lukashin<sup>1</sup>, Yuri D. Tretyakov<sup>1</sup>, and Peter Goernert<sup>2</sup>

<sup>1</sup>Department of Materials Science, Moscow State University, Moscow, 119992, Russia; <sup>2</sup>INNOVENT, Prüssingstrasse 27 B, D-07745 Jena, Germany

**Abstract:** Here we report the synthesis and investigation of cobalt nanowire arrays using mesoporous silica as a host material. In the present work, a novel variant of synthesis of ordered magnetic nanowires in the mesoporous silica matrix was suggested. The method is based on incorporation of a hydrophobic metal compound  $\text{Co}_2(\text{CO})_8$  into the hydrophobic part of the silica-surfactant composite. The amount of cobalt intercalated into the mesoporous matrix was measured by chemical analysis (~5 wt %). Additional thermal modification was performed in order to provide a crystallization process of the cobalt nanowires. The prepared nanocomposites were characterized by X-ray diffraction (XRD), small-angle X-ray spectroscopy (SAXS), transmission electron microscopy (TEM), nitrogen capillary adsorption method (BET and BJH), and magnetic measurements. The anisotropy parameters of nanowires were determined using temperature dependence of magnetic susceptibility. For cobalt-containing sample annealed at 300 °C (form factor of nanowire higher than 16), the coercive force at room temperature was found to be 42.2 kA/m at saturation magnetization of 0.5 A·m<sup>2</sup>/kg, which is nearly sufficient for modern information recording media. According to TEM studies, cobalt particles are uniform and well ordered in the silica matrix. Thus, the suggested method leads to one-dimensional anisotropic nanostructures, which could find an application in high-density data storage devices.

**Keywords:** nanocomposites; magnetic nanowires; cobalt; mesoporous silica; anisotropy; ordered nanowire arrays; magnetic data storage.

### INTRODUCTION

Ordered nanostructure arrays have attracted close attention of researchers all over the world due to their great potential in tailoring functional properties of materials for various practical applications [1]. One of the major problems in materials science is connected with development of ordered magnetic nanoparticle arrays as a medium for modern magnetic data storage devices with ultra-high density of recording [2,3]. It is well known that the possibility of storing one bit of information on a single nanoparticle enables the colossal growth of storage capacities [2,4]. However, decreasing particle size to atomic scale results in superparamagnetic behavior of magnetic nanostructures (with zero coercivity) due to temperature-induced fluctuations of the magnetic moment [3]. To get over the “superparamagnetic limit”, one

\*Paper based on a presentation at the 3<sup>rd</sup> IUPAC Workshop on Advanced Materials (WAM III), Stellenbosch, South Africa, 5–9 September 2005. Other presentations are published in this issue, pp. 1619–1801.

‡Corresponding author: Fax +7-(095)-939-0998; E-mail: eliseev@inorg.chem.msu.ru

should increase system magnetic energy, which is represented by exchange interactions, magneto-elastic, magnetocrystalline, and magnetostatic (demagnetization) energies. Thus, increasing the coercive force of nanoparticles is achievable by increasing any of these components. From a theoretical point of view, the fixation of the magnetic moment of particles can easily be reached by inducing the magnetocrystalline anisotropy of the material [5]. Magnetic media with high crystal cell anisotropy are characterized by magnetization vectors aligned in a certain crystallographic direction (i.e., easy magnetization axis) due to the spin-orbital interactions. Another pathway for fastening of the magnetic moment in nanoparticulate media involves the formation of strongly anisotropic nanoparticles, which could certainly increase blocking temperature and coercivity of the medium [6]. Magnetic shape anisotropy appearing in wire-like particles aligns magnetization vector parallel to the long axis of a wire and provides rather high coercivity value even for small particle diameters. The higher the form factor of the nanostructure, the higher is the blocking temperature and coercive force of the system at constant volume of nanoparticle. For example, the approach to increase coercivity for iron nanoparticles was successfully accomplished earlier by inducing their shape anisotropy (at diameter  $\sim 1$  nm), which resulted in ferromagnetic behavior of the system at room temperature with maximal coercivity of 35 kA/m [7]. The wires were synthesized in the mesoporous silica channels by intercalation of a hydrophobic iron compound  $\text{Fe}(\text{CO})_5$  into a hydrophobic part of the silica-surfactant composite followed by a chemical modification of the complex. It is believed that increasing the magnetocrystalline energy of the medium by replacing Fe for any anisotropic material, with easy magnetization axes aligned parallel to the long wire dimension, will lead to the noticeable increase of the coercivity of the magnetic medium. At the same time, hexagonal cobalt phase (*hcp*) is characterized by magnetocrystalline anisotropy constant value  $K_1$  of  $7 \cdot 10^5$  J/m<sup>3</sup> and, therefore, by enhanced coercivity as compared to iron [8].

Therefore, the present study is focused on the development of cobalt nanostructure arrays possessing high anisotropy of the particles. From the synthetic point of view, the synthesis of highly anisotropic nanostructures usually involves the use of geometrically confined systems at nanolevel as a reactor for preparation or crystallization of particles [9]. At the same time, the application of nanostructures as magnetic materials requires their rigid fixation. This could be achieved by encapsulation of nanoparticles in a chemically inert matrix. Such an approach enables one to avoid aggregation of particles and protect them from the effect of external factors, and, therefore, makes it possible to take advantage of the specific properties of nanomaterials [10]. The methods of matrix isolation can be divided into two groups: synthesis of free nanoparticles followed by their incorporation into a matrix and direct formation of nanostructures in structural cavities or in a pore system of porous medium by chemical modification of intercalated compounds [9]. The second group makes it possible to control directly the shape of nanoparticles formed. In this case, pore walls confine the reaction zone during chemical modification, i.e., they serve as solid-state nanoreactors. One can expect the size and shape of nanoparticles produced in nanoreactors to be consistent with the dimensions of the porous framework. Thus, the major point for the development of well-ordered nanowire arrays is the choice of an appropriate matrix.

One of the most promising matrices for the preparation of highly anisotropic nanoparticle arrays are mesoporous phases with hexagonal arrangement of cylindrical pores, possessing very high length of the mesopore channel and very low diameter (the pore diameter can be controllably varied from 2 to 50 nm) [11]. These pore systems have maximal anisotropy constants and could be considered as one-dimensional [11]. Hexagonal mesoporous silica phases have been widely used as solid-state nanoreactors for the preparation of metal and metal oxide nanowires [12], polymer fibers [13], carbon nanotubes [14], etc. In these studies, the walls of mesoporous silica channels were used as spatial separators, preventing diffusion of reactants or aggregation of nanostructures formed and restraining their interaction with atmosphere.

The application of magnetic nanowire arrays confined in the mesoporous silica channels as data storage medium implies the realization of longitudinal recording scheme, since the channels of mesoporous silica are known to align parallel to the substrate to minimize the free energy of the system

(Fig. 1). The formation of mesoporous silica films with a highly aligned system of mesochannels parallel to the substrate plane was reported recently on Si(110) substrate [15]. In case of encapsulation of a magnetic material into the pores, one will get a perfect system of isolated nanomagnets inside the diamagnetic matrix. The main advantage of this approach is the presence of the ordered array of magnetic domains, which enables precise positioning of the writing/reading head while writing or reading.

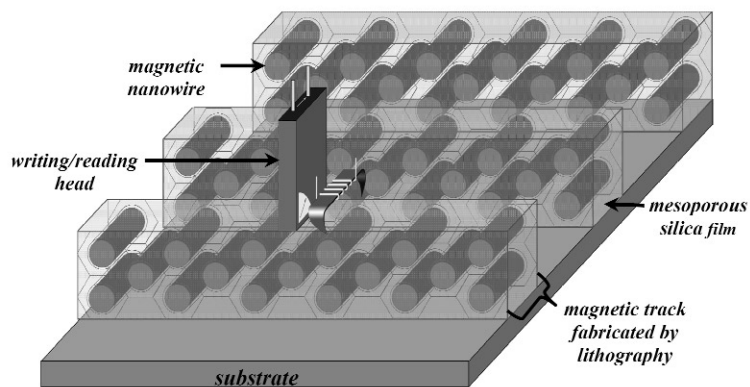


**Fig. 1** Scheme of high-density data storage devices based on magnetic nanowires in the mesoporous silica films.

Recent investigations in the field of the preparation of cobalt nanoparticles in mesoporous silica matrix are basically focused on catalytic applications, including a wide range of heterogeneous catalytic reactions like selective oxidation of aromatic hydrocarbons, alkanes, and alkenes, process of CO conversion, reduction of  $\text{NO}_x$ , synthesis of higher hydrocarbons, gasoline, and synthesis gas, etc. [16,17]. To date, a number of incorporation techniques were developed, including impregnation by the solutions of cobalt salts or complexes (e.g., nitrate, chloride, acetate, oxalate, acetylacetonate, or carbonyl) [16–18], in situ intercalation of metal (one-step synthesis) [16,19], chemical vapor disposition (CVD) processing [20], etc. However, impregnation techniques usually lead to the formation of relatively large nanoparticles exceeding the size of the pores. The reason for the formation of nanoparticles outside the pores is high mobility of cations through silanol OH-groups. CVD of a volatile cobalt compound resulted in nonhomogeneous distribution of particles due to partial blocking of the mesopore channels. The same result was observed for electrochemical deposition of cobalt or intercalation of presynthesized cobalt nanoparticles in tri-*n*-octylphosphine oxide (TOPO) shell [21]. The works on chemical bonding of cobalt by functional groups grafted on silica surface do not describe the temperature modification of synthesized composites [22]. Only a few studies report magnetic properties of nanosized cobalt particles in MCM-41 and SBA-15 matrices [23]. However, X-ray diffraction (XRD) analysis of these composites revealed the formation of cubic cobalt phase.

Here we used another approach based on the intercalation of a hydrophobic metal compound (cobalt carbonyl) into the hydrophobic part of the as-prepared mesoporous silica-surfactant composite. This method was applied earlier for the formation of iron nanowires with a characteristic width of 1–2 nm and length over 100 nm [24].

## EXPERIMENTAL DETAILS

The mesoporous silica matrix (**MCM-41**) was obtained by polycondensation of tetraethylorthosilicate (TEOS, 98 %, Aldrich) in the aqueous template solution ( $\text{C}_{16}\text{H}_{33}(\text{CH}_3)_3\text{NBr}$ , Aldrich 99 %) with the following molar ratio of reactants: 1 TEOS:0.152  $\text{C}_{16}\text{H}_{33}(\text{CH}_3)_3\text{NBr}$ :2.8  $\text{NH}_3$ :141.2  $\text{H}_2\text{O}$  [25]. In order to perform introduction of cobalt into the silica matrix, we have chosen dicobalt octacarbonyl because

this nonpolar molecule can be expected to dissolve well in the hydrophobic part of the SiO<sub>2</sub>/surfactant micelles and is easily decomposed to give elemental cobalt [26]. The intercalation of Co<sub>2</sub>(CO)<sub>8</sub> into MCM-41 was carried out by soaking ~2 g of dried matrix with 0.075 M solution of cobalt carbonyl in mesitylene (prepared by dissolving 1.2 g Co<sub>2</sub>(CO)<sub>8</sub> in 46 ml of mesitylene), for 24 h in Ar atmosphere at room temperature. Impregnated sample was washed by mesitylene to get rid of Co<sub>2</sub>(CO)<sub>8</sub> absorbed on the external surface. The decomposition of cobalt carbonyl was achieved by UV-irradiation of composite (DRT-1000 lamp, 1000 W) for 3 h, followed by crystallization in H<sub>2</sub> flow at elevated temperatures (300–700 °C) for 3 h. Obtained samples were denoted as Co/SiO<sub>2</sub>-*T*, where *T* is crystallization temperature.

The samples were investigated by powder XRD (Siemens D5000, CuK<sub>α1</sub> radiation, λ<sub>wave</sub> = 1.54 Å, 2θ scan step 0.05°, 2θ range 5–65°), small-angle X-ray scattering (SAXS, Scintag 2000 diffractometer, 20 kV, 5 mA, Cu K<sub>α1</sub> radiation, 2θ scan step 0.02°), nitrogen capillary adsorption method (COULTER™ SA 3100™, working gas N<sub>2</sub>, 77 K), chemical analysis (Optima 5300 DV, Perkin Elmer), transmission electron microscopy (TEM, JEM-2000FXII, JEOL, acceleration voltage 200 kV), and magnetic measurements (S600 SQUID magnetometer, APD Cryogenics).

## RESULTS AND DISCUSSION

According to SAXS experiments, mesoporous silica matrix possesses highly ordered hexagonal arrangement of pores with the lattice *a* parameter of 4.7 nm and *d*<sub>100</sub> spacing of 4.1 nm (Fig. 2). Nitrogen capillary adsorption studies of annealed mesoporous matrix (550 °C, 1 °C/min, O<sub>2</sub>) show very high specific surface area of 1240 m<sup>2</sup>/g and average pore diameter of 2.9 nm that is in good agreement with literature data.

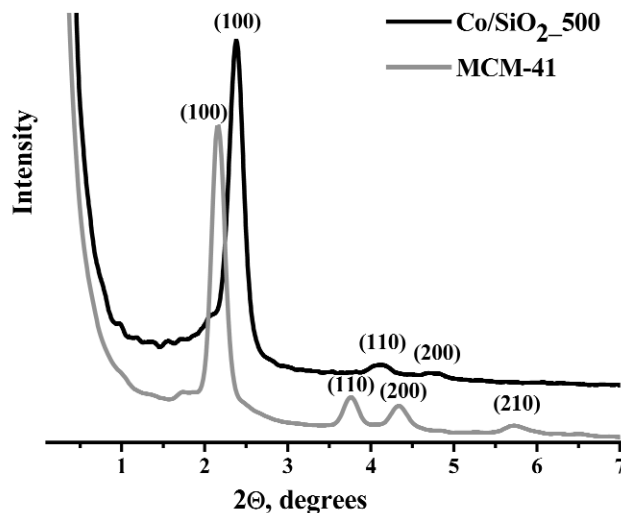


Fig. 2 SAXS data for pure MCM-41 matrix and Co/SiO<sub>2</sub>-500 nanocomposite.

To prove the presence of mesoporous structure after intercalation of cobalt, SAXS experiments for Co/SiO<sub>2</sub> nanocomposite crystallized at 500 °C and as-prepared mesoporous silica matrix were performed. The comparison between SAXS patterns for the samples designates that the decomposition of cobalt carbonyl did not bring considerable influence on the porous structure (Fig. 2). However, the position of (100), (110), and (200) reflections for annealed sample shifted toward higher 2θ values, indi-

cating the decrease of  $a$  lattice parameter from 4.7 to 4.3 nm (**Co/SiO<sub>2</sub>\_500**), which is attributed to shrinking of mesoporous silica structure at high temperatures.

The removal of template molecules after reduction in hydrogen was verified by the method of capillary absorption of nitrogen at 77 K (CTAB decomposition temperature is 230 °C). According to Brunauer–Emmett–Teller (BET) and Barret–Joyner–Halenda (BJH) analysis, annealing of the samples at temperatures exceeding 300 °C leads to the formation of open porous structure with high surface areas and specific step-like increase in absorbance curve at  $\sim 0.3 P_S/P_0$ . The increase of the annealing temperature is accompanied by a slight increase of surface area values (from 820 m<sup>2</sup>/g for **Co/SiO<sub>2</sub>\_300** to 910 m<sup>2</sup>/g for **Co/SiO<sub>2</sub>\_500**) and BJH pore diameter (from 2.8 nm for **Co/SiO<sub>2</sub>\_300** to 3.0 nm for **Co/SiO<sub>2</sub>\_500**), which can be ascribed to evaporation of residual carbon.

The amount of cobalt intercalated into the mesoporous matrix was measured by chemical analysis. Slight reduction of cobalt content from 5.3 wt % for **Co/SiO<sub>2</sub>\_300** composite to 4.7 wt % for **Co/SiO<sub>2</sub>\_500** demonstrates partial sublimation of cobalt polycarboniles formed after UV-irradiation. Rather low Co loading value indicates that cobalt particles could not wholly fill the pore structure, which could result in either inhomogeneous distribution of metal along the channels or in the formation of small-diameter (around 1 nm) particles coordinated to the inner surface of pores (in this case, the nonhomogeneity will appear in a direction perpendicular to the long axis of the pore structure). The first case will lead obviously to partial blocking of mesopore channels with Co clusters, which will drastically reduce the surface area of the composites. In the second case, the system will possess open porous structure, as observed by surface analysis.

XRD studies of **Co/SiO<sub>2</sub>\_T** series indicate no formation of any macrocrystalline phases until 700 °C, while further increase of the annealing temperature results in the appearance of cubic Co reflections ( $d_{111} = 2047$  Å and  $d_{200} = 2177$  Å reflections, ICDD, No. 15-0806). Obviously, raising the annealing temperature of nanocomposites leads to increasing the mobility of cobalt atoms, resulting in aggregation and formation of large particles outside mesoporous channels. Unfortunately, XRD gives no information on the composition of cobalt-containing phases (oxides, *hcp* or *fcc* phases), which probably deals with formation of nanoparticles with average size below 5 nm. This suggests the formation of cobalt-containing particles inside mesoporous structure and the absence of large particles on the external surface. On the other hand, bulk cobalt is known to have *hcp*  $\rightarrow$  *fcc* phase transformation point at  $\sim 425$  °C, making composites obtained below 425 °C of special interest [27].

The direct TEM observations of nanocomposites proves the presence of hexagonally ordered porous structure with interpore distances of  $\sim 4$  nm, which is in good agreement with  $a$  parameter of MCM-41 unit cell (Figs. 3a,b). TEM images of **Co/SiO<sub>2</sub>\_300** composite reveal the absence of large particles on the surface of mesoporous silica crystallites, while higher reduction temperatures demonstrate partial emergence of cobalt atoms from silica channels with formation of spherical particles with an average diameter of  $\sim 5$  nm (Figs. 3a–c). Unfortunately, electron diffraction studies show no crystalline phases in the composites due to the rather small size of cobalt-containing particles.

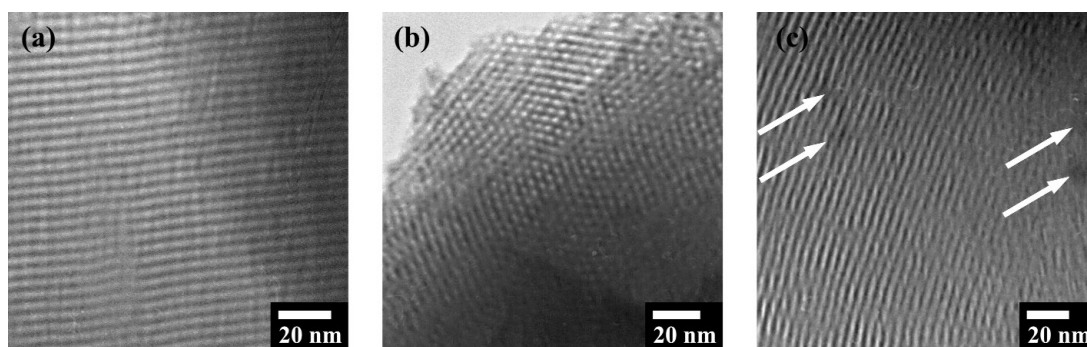


**Fig. 3** TEM images for composites  $\text{Co/SiO}_2\text{-300}$  (a, b) and  $\text{Co/SiO}_2\text{-350}$  (c).

The most important parameter of the obtained system is anisotropy of nanoparticles. Unfortunately, it could not be determined by direct electron microscopy studies since the boundary between adjacent particles could not be clearly seen. Therefore, the anisotropy parameters of the magnetic particles were calculated using the temperature dependence of the magnetic susceptibility. The measurements for field-cooled (FC) and zero-field-cooled (ZFC) samples were carried out in the temperature range 2–300 K (Fig. 4). All samples demonstrate ferromagnetic or superparamagnetic behavior, with blocking temperature of  $\sim 300$  K (Table 1). The blocking temperature was calculated as a point of 10 % difference between magnetization of FC and ZFC samples. One can see that blocking temperature tends to decrease with increasing of crystallization temperature (Table 1). In accordance with the open porous structure of composites (the specific surface areas attain  $900 \text{ m}^2/\text{g}$ ) the formation of array of small particles on the inner surface of pores was assumed. Obviously, these particles form joint magnetically correlated cylindrical volumes (or nanowires). In this case, blocking temperatures and the size of magnetically ordered volumes are determined by the longitudinal dimension of magnetic nanowires at constant diameter of a single wire, which could be obtained by TEM. This enables us to calculate the length of the wires using the following formula:

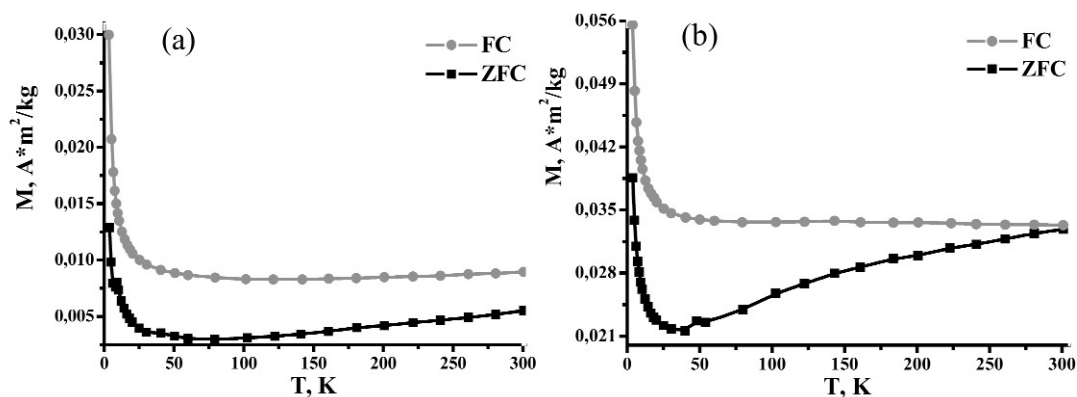


**Fig. 4** Temperature dependences of magnetic susceptibility for composites  $\text{Co/SiO}_2\text{-}T$  obtained at  $300^\circ\text{C}$  (a) and  $500^\circ\text{C}$  (b).

**Table 1** Magnetic properties of **Co/SiO<sub>2</sub>-T** nanocomposites.

Sample	Blocking temperature, K	Form-factor of Co nanowires	Coercivity, kA/m		Magnetization at field 795.8 kA/m, 300 K (A·m <sup>2</sup> /kg)
			4K	300K	
<b>Co/SiO<sub>2</sub>-300</b>	>300	>16	8.0	42.2	0.50
<b>Co/SiO<sub>2</sub>-350</b>	300	16	11.9	35.0	0.63
<b>Co/SiO<sub>2</sub>-400</b>	300	16	14.3	23.9	0.71
<b>Co/SiO<sub>2</sub>-500</b>	210	11	20.7	14.3	1.0

$$T_B = \frac{\Delta E}{k \ln(\tau \cdot f_0)} \approx \frac{\left[ 0.25 \cdot I_s^2 (N_{\parallel} - N_{\perp}) + K_1 \right] \cdot V}{25k} \quad (1)$$

where  $\Delta E$  is activation barrier,  $\tau$  is the relaxation time,  $f_0$  is the frequency factor,  $N_{\perp}$  and  $N_{\parallel}$  are the demagnetization coefficients perpendicular and along the axes of easy magnetization,  $I_s$  is the saturation magnetization,  $K_1$  is the magnetic anisotropy constant, and  $V$  is the particle volume.

As blocking temperature of samples attain 300 K, the parameters of anisotropy for magnetic domains exceed 16. Therefore, decomposition of cobalt carbonyl in the spatially constrained reaction zone of mesoporous system cause the formation of anisotropic cobalt particles with diameter of 1–2 nm and length over 16 nm. One should note that high anisotropy constants of nanoparticles should result in high coercivity of composites due to the increase of demagnetization field with increasing length/diameter ratio. The magnetic properties of **Co/SiO<sub>2</sub>-T** nanocomposites are summarized in Table 1. Magnetization dependence on the external magnetic field at 300 K demonstrates growth of saturation magnetization (magnetization at 795.8 kA/m) with annealing temperature, which indicates crystallization of cobalt particles (Fig. 5). At the same time, the coercivity of the composites has an opposite tendency, which is probably attributed to destruction of Co nanowires (with reduce of anisotropy parameter) due to the increase of cobalt atom mobility at elevated temperatures. The decrease of blocking temperature and coercive force for **Co/SiO<sub>2</sub>-500** sample can also be explained by the transformation of Co from the hexagonal to cubic phase. The maximal coercivity values for **Co/SiO<sub>2</sub>-T** samples attain 42.2 kA/m at room temperature, which is nearly sufficient for modern magnetic data storage.

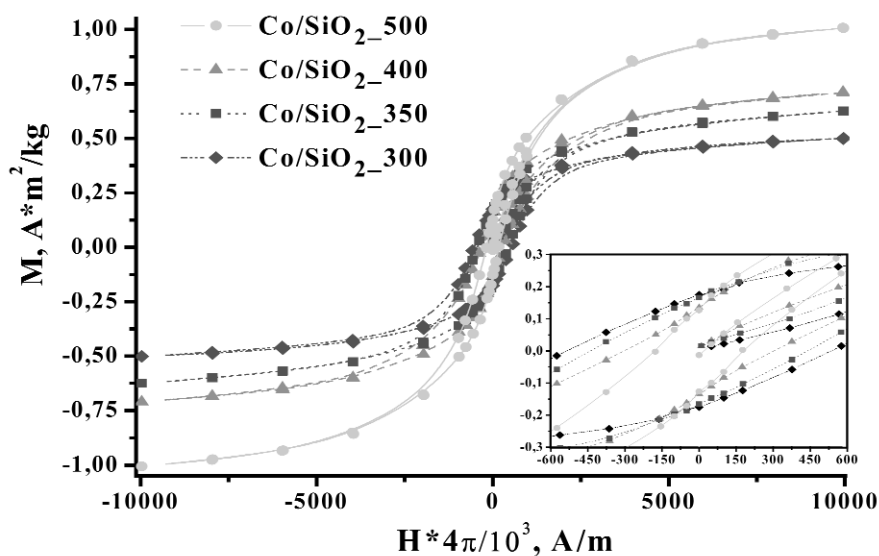


Fig. 5 Hysteresis loops of  $\text{Co/SiO}_2\text{-}T$  samples studied at 300 K.

## CONCLUSIONS

Thus, in the present study, we successfully realized a novel variant of the synthesis of ordered magnetic cobalt nanowires in the mesoporous silica matrix by incorporation of a hydrophobic metal complex  $\text{Co}_2(\text{CO})_8$  into the hydrophobic part of the as-prepared  $\text{SiO}_2$ /surfactant composite followed by decomposition of complex and crystallization of Co particles. The proposed method enables us to control the anisotropy and magnetic properties of nanostructures formed in the mesoporous silica matrix. It also allows us to achieve the formation of highly anisotropic nanostructures with ferromagnetic properties at room temperature.

## ACKNOWLEDGMENTS

This work is supported by the scientific program “Universities of Russia” (06.02.031), RFBR (03-03-32182), INTAS (01-204 and 03-55-1523), grant from Foundation of National Science Support. The authors also would like to acknowledge the help of Dr. Alexandr V. Knotko for TEM imaging and Dr. Artem P. Malakho for SAXS experiments.

## REFERENCES

1. A. S. Edelstein, R. C. Cammarata (Eds.). *Nanomaterials: Synthesis, Properties and Applications*, Institute of Physics Publishing, Bristol (1997).
2. A. K. Menon, B. K. Gupta. *Nanostruct. Mater.* **11**, 965 (1999).
3. D. A. Thompson, J. S. Best. *IBM J. Res. Dev.* **44**, 311 (2000).
4. A. A. Eliseev, I. V. Kolesnik, A. V. Lukashin, Y. D. Tretyakov. *Adv. Eng. Mater.* **7**, 213 (2005).
5. N. A. Spaldin (Ed.). *Magnetic Materials. Fundamentals and Device Applications*, Cambridge University Press, Cambridge (2004).
6. G. M. Chow, K. E. Gonsalves (Eds.). *Nanotechnology: Molecularly Designed Materials*, American Chemical Society, Washington, DC (1996).
7. A. A. Eliseev, K. S. Napolskii, A. V. Lukashin, Yu. D. Tretyakov. *J. Magn. Magn. Mater.* **272**, 1609 (2004).

8. D. L. Leslie-Pelecky, R. D. Rieke. *Chem. Mater.* **8**, 1770 (1996).
9. Yu. D. Tretyakov, A. V. Lukashin, A. A. Eliseev. *Russ. Chem. Rev.* **73**, 974 (2004).
10. K. J. Kirk. *Contemp. Phys.* **41**, 61 (2000).
11. J. S. Beck, J. C. Vartuli, W. J. Roth, M. E. Leonowicz, C. T. Kresge, K. D. Shmitt, C. T. W. Chu, D. H. Olson, E. W. Sheppard, S. B. McCullen, J. B. Higgins, J. L. Schlenker. *J. Am. Chem. Soc.* **114**, 10834 (1992).
12. C. N. R. Rao, F. L. Deepak, G. Gundiah, A. Govindaraj. *Prog. Solid State Chem.* **31**, 5 (2003).
13. K. Tajima, T. Aida. *Chem. Commun.* **24**, 2399 (2000).
14. A. B. Fuertes. *Microporous Mesoporous Mater.* **67**, 273 (2004).
15. M. Hirokatsu, K. Kazuyuki. *J. Am. Chem. Soc.* **33**, 7618 (1999).
16. J. E. Haskouri, S. Cabrera, C. J. Gomez-Garcia, C. Guillem, J. Latorre, A. Beltran, D. Beltran, M. D. Marcos, P. Amoros. *Chem. Mater.* **16**, 2805 (2004).
17. B. Ernst, S. Libs, P. Chaumette, A. Kiennemann. *Appl. Catal., A* **186**, 145 (1999).
18. J. Panpranota, S. Kaewkuna, P. Prasertdama, J. G. Goodwin. *Catal. Lett.* **91**, 95 (2003).
19. A. M. Tshavhungwe, N. J. Coville. *J. Sol-Gel Sci. Technol.* **31**, 161 (2004).
20. S. Suvanto, J. Hukkamaki, T. T. Pakkanen, T. A. Pakkanen. *Langmuir* **16**, 4109 (2000).
21. A. F. Gross, M. R. Diehl, K. C. Beverly, E. K. Richman, S. H. Tolbert. *J. Phys. Chem. B* **107**, 5475 (2003).
22. M. Nowotny, L. N. Pedersen, U. Hanefeld, T. Maschmeyer. *Chem. Eur. J.* **8**, 3724 (2002).
23. H. Luo, D. Wang, J. He, Y. Lu. *J. Phys. Chem. B* **109**, 1919 (2005).
24. K. S. Napolsky, A. A. Eliseev, A. V. Knotko, A. V. Lukashin, A. A. Vertegel, Yu. D. Tretyakov. *Mater. Sci. Eng., C* **23**, 151 (2003).
25. M. Grun, K. K. Unger, A. Matsumoto, K. Tsutsumi. *Microporous Mesoporous Mater.* **27**, 207 (1999).
26. V. G. Sirkin. *Karbonilnie Metalli*, pp. 5–27, Metallurgiya, Moscow (1978) (in Russian).
27. E. P. Wohlfarth (Ed.). *Ferromagnetic Materials*, pp. 1–70, North-Holland, Amsterdam (1980).